INTERNATIONAL JOURNAL FOR NUMERICAL METHODS IN FLUIDS, VOL. 4, 399–419 (1984)

A DORODNITSYN FINITE ELEMENT FORMULATION FOR LAMINAR BOUNDARY LAYER FLOW

C. A. J. FLETCHER AND R. W. FLEET

Department of Mechanical Engineering, University of Sydney, Sydney, NSW 2006, Australia

SUMMARY

The Dorodnitsyn boundary later formulation is given a finite element interpretation and found to generate very accurate and economical solutions when combined with an implicit, non-iterative marching scheme in the downstream direction. The algorithm is of order $(\Delta^2 u, \Delta x)$ whether linear or quadratic elements are used across the boundary layer. Solutions are compared with a Dorodnitsyn spectral formulation and a conventional finite difference formulation for three Falkner–Skan pressure gradient cases and the flow over a circular cylinder. With quadratic elements the Dorodnitsyn finite element formulation is approximately *five times more efficient* than the conventional finite difference formulation.

KEY WORDS Laminar Boundary Layers Finite Element Method Finite Difference Method Spectral Method Convergence Computational Efficiency

1. INTRODUCTION

In the past boundary layer flows have been computed effectively with both finite difference formulations[1,2] and finite element formulations.[3–5] Generally a solution is sought in terms of the velocity components, u and v, as functions of x and y, in two dimensions.

The Dorodnitsyn[6] boundary layer formulation (method of integral relations) is known to obtain relatively accurate solutions with only a few (3 or 4) coefficients defining the velocity profile across the boundary layer. In part the high accuracy comes from treating u as an independent, rather than a dependent, variable. Here we propose to combine the Dorodnitsyn formulation with *finite element* procedures to see if a computationally more efficient algorithm can be developed for general boundary layer flows.

The method of integral relations[7] can be interpreted as a method of weighted residuals[8] in which a partial differential equation is reduced to a system of ordinary differential equations.

Suppose a system of a partial differential equations is written

$$\sum_{i=1}^{n} \frac{\partial P_m}{\partial x_i} - F_m = 0 \tag{1}$$

where P_m and F_m are known functions of the dependent variables, u_i. The method of integral relations replaces equation (1) with

$$\int_{\substack{x_i \\ i \neq j}} f_k \left(\sum_{i=1}^{n} \frac{\partial P_m}{\partial x_i} - F_m \right) \mathrm{d}x_i = 0 \tag{2}$$

0271–2091/84/050399–21$02.10

Received 29 September 1982
Revised 11 February 1983

Equation (2) is a system of ordinary differential equations in the x_jth $(i \neq j)$ co-ordinate direction and f_k is a family of weight functions.

If f_k were chosen as Dirac delta functions centred at the nodal points in the x_ith $(i \neq j)$ co-ordinate directions the same system of ordinary differential equations would result as by replacing appropriate derivatives in equation (1) with finite difference formulae. However the utility of the method of integral relations (MIR) is demonstrated better by choosing *smooth* functions for f_k. Then solutions of high accuracy can be obtained with relatively few unknown in the x_ith $(i \neq j)$ directions.

The method of integral relations (MIR) is particularly effective for parabolic problems that can be reduced to ordinary differential equations in the time or time-like direction. Dorodnitsyn[6] developed a *particular* method of integral relations for the boundary layer equations and that will be the starting point for this paper.

If the weight function, f_k, in equation (2) is chosen to coincide with the analytic functions used to represent u_i a Galerkin method[8] is obtained. For certain classes of problems the Galerkin method is optimal.

It has been found[9,10] that by modifying the Dorodnitsyn method of integral relations to make use of orthonormal weight and approximating functions a Galerkin formulation is produced. This will be referred to as the *Dorodnitsyn spectral formulation* in this paper.

The Galerkin finite element method has proved to be a *particularly efficient* interpretation of the Galerkin formulation. In common with the method of integral relations or the method of weighted residuals, the finite element method obtains more accurate solutions by combining a smooth weight (or test) function with the integral (weak) formulation, equation (2). By using *local* test functions the finite element method can be combined more efficiently with the numerical integration procedure for the time or time-like co-ordinate direction.

Consequently the main purpose of this paper is to interpret the Dorodnitsyn boundary layer formulation *in a finite element context.* The result is an algorithm that is both highly accurate and economical.

The alternative Dorodnitsyn formulations, traditional MIR, orthonormal (spectral) MIR and the Dorodnitsyn finite element method, are described in Section 2—with reference to the two-dimensional, laminar incompressible boundary layer equations.

The convergence properties of the Dorodnitsyn finite element formulation are examined in Section 3 for linear and quadratic shape functions in u. The Falkner–Skan class of similar solutions can be computed very accurately. These solutions have been used to test the convergence of T (equation (25)) in the L_2 norm. The convergence rates for both varying Δu and Δx have been considered. The convergence behaviour in the '*engineering*' norms, skin friction, displacement and momentum thickness, has also been established.

The computational efficiency of the Dorodnitsyn finite element formulation is compared with that of a conventional finite difference formulation in Section 4 for the Falkner–Skan problems. By computational efficiency we will understand the accuracy achieved for a given execution (CPU) time.

The Dorodnitsyn finite element method is compared with a finite difference method and the Dorodnitsyn spectral method, for the boundary layer flow over a circular cylinder, in Section 5. This problem is a good test of the method since it combines a region of favourable pressure gradient with a region of adverse pressure gradient terminating in the separation of the boundary layer.

The extension of the Dorodnitsyn finite element method to solve turbulent boundary layer problems and a comparison with the Dorodnitsyn spectral formulation and a representative finite difference method STAN5, is described by Fletcher and Fleet.[11]

2. ALTERNATIVE DORODNITSYN FORMULATIONS

To clarify the description of the method we will restrict our attention to the two-dimensional, incompressible laminar boundary layer equations,

$$u_x + v_y = 0 \tag{3}$$

and

$$uu_x + vu_y = u_e u_{ex} + \frac{1}{Re} u_{yy} \tag{4}$$

Initial conditions are provided at $x = x_0$ by

$$u(x_0, y) = u_i(y) \quad \text{and} \quad v(x_0, y) = v_i(y)$$

with $u_i(y)$, $v_i(y)$ known. Boundary conditions are

$$u(x, 0) = v(x, 0) = 0 \quad \text{and} \quad u(x, \infty) = u_e(x) \tag{5}$$

$u_e(x)$ in equations (4) and (5) is the known velocity distribution at the outer edge of the boundary layer. In equations (3)–(5) u,v and u_e have been non-dimensionalized with respect to a reference velocity, u_∞, and x and y with respect to a reference length, L. The Reynolds number, Re, is given by

$$Re = u_\infty L/\nu$$

where ν is the kinematic viscosity.

In this section the traditional Dorodnitsyn formulation of equations (3)–(5) will be described first. Improvements to this method that generate a spectral (orthonormal) formulation and a finite element formulation will be described subsequently.

2.1. *Traditional Dorodnitsyn formulation*

Dorodnitsyn[6] applied the method of integral relations (MIR) to the boundary layer equations, (3)–(5), in a particularly novel manner. Previous applications of MIR had been restricted to inviscid (and usually compressible) flow. The development of MIR is described comprehensively by Holt.[7]

The traditional Dorodnitsyn boundary layer formulation can be introduced as follows. Let

$$\xi = \int_0^x u_e(x')\,dx', \qquad \eta = Re^{1/2} u_e y$$

$$u' = u/u_e, \qquad v' = Re^{1/2} v/u_e \quad \text{and} \quad w = v' + \eta u' u_{e\xi}/u_e$$

Equations (3) and (4) become

$$u'_\xi + w_\eta = 0 \tag{6}$$

$$u'u'_\xi + wu'_\eta = \frac{u_{e\xi}}{u_e} + u_{\eta\eta} \tag{7}$$

with boundary conditions,

$$u' = w = 0 \quad \text{at} \quad \eta = 0, \qquad u' = 1 \quad \text{at} \quad \eta = \infty \tag{8}$$

A general weight function, $f(u')$, is introduced and the following product formed

$$f \times \text{equation (6)} + f_{u'} \times \text{equation (7)} = 0$$

The result is (dropping the superscript $'$ from u')

$$(uf)_\xi + (wf)_\eta = \frac{u_{e\xi}}{u_e} f_u(1-u^2) + f_u u_{\eta\eta} \tag{9}$$

Equation (9) is integrated with respect to η to give

$$\frac{\partial}{\partial \xi}\int_0^\infty uf\,\mathrm{d}\eta + [wf]_0^\infty = \frac{u_{e\xi}}{u_e}\int_0^\infty f_u(1-u^2)\,\mathrm{d}u - [f_u u_\eta]_{\eta=0} - \int_0^\infty f_{uu}(u_\eta)^2\,\mathrm{d}\eta \tag{10}$$

If there is no surface injection in the problem ($w = 0$ at $\eta = 0$) and $f(u)$ is chosen to vanish at $\eta = \infty$ then w and v' do not appear explicitly in the formulation.

If we define $\mathrm{T} = 1/\Theta = u_\eta$ and change the variable of integration in equation (10) from η to u, the result is

$$\frac{\partial}{\partial \xi}\int_0^1 uf\Theta\,\mathrm{d}u = \frac{u_{e\xi}}{u_e}\int_0^1 f_u(1-u^2)\Theta\,\mathrm{d}u - [f_u \mathrm{T}]_{u=0} - \int_0^1 f_{uu}\mathrm{T}\,\mathrm{d}u = 0 \tag{11}$$

Equation (11) is the Dorodnitsyn boundary layer formulation. The *dependent variables* are Θ and T and the *independent variables* are ξ and u.

The Dorodnitsyn formulation offers a number of *significant* advantages for boundary layer computation. Firstly an infinite domain in the y direction is replaced by a *finite* domain in the u direction. A *uniform* grid in u automatically captures downstream boundary layer growth and provides *high resolution* (in physical space) close to the wall. For typical velocity distributions across the boundary layer, this aspect is illustrated in Figure 1. The high resolution near the wall is even more important for turbulent boundary layers.[11]

Since w and v do not appear explicitly in equation (11) only one equation need be solved. The normal velocity, v, can be recovered subsequently if required. Since, in the Dorodnitsyn formulation, $\mathrm{T}(=\partial u/\partial \eta)$ is solved for directly, the calculation of skin friction is *particularly accurate.*

For the traditional Dorodnitsyn formulation the u dependence of Θ and T is approximated as follows

$$\Theta = \frac{1}{(1-u)}(b_0 + b_1 u + b_2 u^2 \ldots b_{N-1}u^{N-1}) \tag{12}$$

and

$$\mathrm{T} = (1-u)(c_0 + c_1 u + c_2 u^2 \ldots c_{N-1}u^{N-1}). \tag{13}$$

The factor $(1-u)$ appearing in equations (12) and (13) is introduced to satisfy the boundary condition $\mathrm{T} = 0$ at $u = 1$. The coefficients, $b_k(\xi)$ and $c_k(\xi)$, are obtained by integrating numerically, in the ξ direction, the system of equations that are obtained by evaluating equation (11) with

$$f_k(u) = (1-u)^k \tag{14}$$

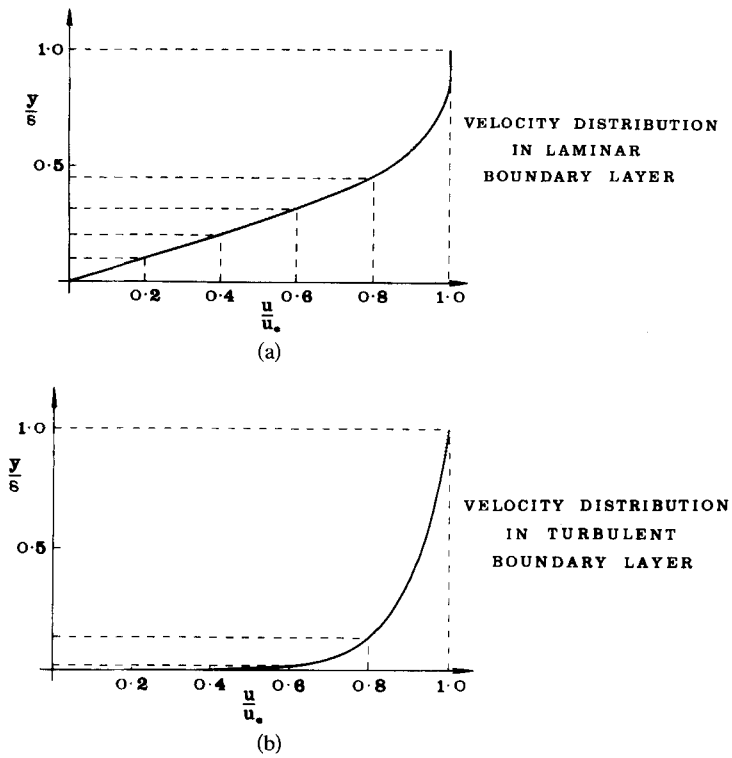

Figure 1. Grid comparison in y and u space

The traditional Dorodnitsyn formulation has proved to be very efficient when *relatively few* terms are used in equations (12) and (13), e.g. $N=2$ to 4. The method has been applied to two and three dimensional, incompressible and compressible, laminar and turbulent boundary layer flows.[7]

2.2. *Dorodnitsyn spectral formulation*

For large values of k in equation (14) the difference between f_k and f_{k+1} becomes very small. Consequently the evaluation of equation (11) produces ordinary differential equations that are almost linearly dependent. As a result the system of ordinary differential equations becomes progressively more *ill-conditioned* as N, in equations (12) and (13), is increased.

The Dorodnitsyn spectral formulation overcomes this problem by replacing the analytic functions u^k in equations (12) and (13) and the weight functions, $f_k(u)$, by related *orthonormal* functions, $g_k(u)$, where

$$g_k(u)=\sum_{r=1}^{k} B_{rk} f_r(u) \tag{15}$$

The coefficients B_{rk} are evaluated using the Gram–Schmidt orthonormalization process[12] so that

$$(g_j, g_k)=\int_0^1 g_j(u)g_k(u)w(u)\,du = 1 \quad \text{if} \quad j=k \tag{16}$$

$$=0 \quad \text{if} \quad j\neq k$$

The appropriate form for $w(u)$ will be indicated below. The trial solution, equation (12), is replaced by

$$\Theta = \frac{1}{(1-u)}\left[b_0 + \sum_{j=1}^{N-1} b_j g_j(u)\right] \tag{17}$$

The non-orthogonal leading term, b_0, is retained so that Θ behaves correctly at the outer edge of the boundary layer.

Substituting equation (17) into equation (11) and replacing f with g gives

$$\frac{\mathrm{d}}{\mathrm{d}\xi}\int_0^1 \left[b_0 + \sum_{j=1}^{N-1} b_j g_j(u)\right] g_k \frac{u}{1-u}\,\mathrm{d}u = C_k \tag{18}$$

where

$$C_k = \frac{u_{e\xi}}{u_e}\int_0^1 \frac{\mathrm{d}g_k}{\mathrm{d}u}(1-u^2)\,\Theta\,\mathrm{d}u - \left[\frac{\mathrm{d}g_k}{\mathrm{d}u}\Big/\Theta\right]_{u=0} - \int_0^1 \frac{\mathrm{d}^2 g}{\mathrm{d}u^2}\Big/\Theta\,\mathrm{d}u$$

and $k = 1, \ldots, N$.

A comparison of equations (16) and (18) indicates that if $w(u) = u/(1-u)$, equation (18) simplifies significantly. Then equation (18) can be written

$$\frac{\mathrm{d}b_0}{\mathrm{d}\xi} V_k + \frac{\mathrm{d}b_k}{\mathrm{d}\xi} = C_k \quad \text{for} \quad k \quad \text{for} \quad k = 1, \ldots, N-1 \tag{19}$$

and

$$\frac{\mathrm{d}b_0}{\mathrm{d}\xi} V_N = C_N \quad \text{for} \quad k = N. \tag{20}$$

Using equation (20), equation (19) can be rewritten

$$\frac{\mathrm{d}b_k}{\mathrm{d}\xi} = C_k - C_N V_k / V_n \tag{21}$$

In equations (19)–(21),

$$V_k = \int_0^1 g_k(u)\frac{u\,\mathrm{d}u}{(1-u)} \tag{22}$$

Clearly the coefficients V_k can be evaluated once and for all.

The system of equations (20) and (21) are integrated very effectively using the variable step, variable order Gear method.[13]

The spectral Dorodnitsyn formulation has been applied to incompressible[9] and compressible[14] laminar flows and to turbulent incompressible flows.[11,15]

2.3. *Dorodnitsyn finite element formulation*

To facilitate the application of the finite element method it is convenient to consider equation (11) in an alternative form.

$$\frac{\partial}{\partial x}\int_0^1 uf\Theta\,\mathrm{d}u = \frac{u_{ex}}{u_e}\int_0^1 f_u(1-u^2)\Theta\,\mathrm{d}u + u_e\int_0^1 f_u \mathrm{T}_u\,\mathrm{d}u = 0 \tag{23}$$

Trial solutions for Θ and T are introduced in the following way

$$\Theta = \sum_{j=1}^{M} N_j(u)/(1-u)\theta_j(x) \tag{24}$$

and

$$\mathrm{T} = \sum_{j=1}^{M} (1-u)N_j(u)\tau_j(x) \tag{25}$$

In equations (24) and (25) N_j are one-dimensional shape functions, either linear or quadratic. The additional factor $(1-u)$ is introduced to ensure the correct behaviour of Θ and T at the outer edge of the boundary layer.

The simultaneous imposition of the particular analytic variation with u within each element on Θ and T prevents the relationship, $\Theta = 1/\mathrm{T}$, being satisfied except at the nodes, i.e. $\theta_j = 1/\tau_j$; or in the limit $M \to \infty$.

The weight function $f_k(u)$ is chosen to be

$$f_k(u) = (1-u)N_k(u) \tag{26}$$

The factor $(1-u)$ in equation (26) is introduced to satisfy the requirement that $f_k(1) = 0$. This ensures that v (or w) does not appear in equation (23).

The substitution of equations (24), (25) and (26) into equation (23) generates a *modified Galerkin* finite element formulation.[8] Evaluation of the various terms produces the following system of ordinary differential equations for θ_j and τ_j:

$$\sum_j CC_{kj}\frac{\mathrm{d}\theta_j}{\mathrm{d}x} = \frac{u_{ex}}{u_e}\sum_j EF_{kj}\theta_j + u_e\sum_j AA_{kj}\tau_j \tag{27}$$

where

$$CC_{kj} = \int_0^1 N_k N_j u\,\mathrm{d}u, \qquad EF_{kj} = \int_0^1 N_j\left\{\frac{\mathrm{d}N_k}{\mathrm{d}u}(1-u) - N_k\right\}(1+u)\,\mathrm{d}u$$

and

$$AA_{kj} = \int_0^1 \left\{\frac{\mathrm{d}N_j}{\mathrm{d}u}(1-u) - N_j\right\}\left\{\frac{\mathrm{d}N_k}{\mathrm{d}u}(1-u) - N_k\right\}\mathrm{d}u$$

The combination of using nodal values, θ_i and τ_i, as unknown and shape functions, N_k, of small support permits an efficient implicit algorithm to be constructed to march the solution in the x direction.

The marching algorithm can be established in the following way. Equation (27) is approximated by

$$\sum_j CC_{kj}\,\Delta\theta_j^{n+1} = \Delta x\{\omega S^{n+1} + (1-\omega)S^n\} \tag{28}$$

where

$$S \equiv \frac{u_{ex}}{u_e}\sum_j EF_{kj}\theta_j + u_e\sum_j AA_{kj}\tau_j$$

and

$$\Delta\theta_j^{n+1} = \theta_j^{n+1} - \theta_j^n$$

the superscript n denotes a particular x location. The parameter ω in equation (28) controls the degree of implicitness. For the results provided in this paper a value $\omega = 0{\cdot}5$ has been used.

In order to construct a linear system of equations for $\Delta\theta_j^{n+1}$, S^{n+1} is linearized about the nth level following the approach of Briley and McDonald,[16]

$$S^{n+1} = S^n + \Delta x \left(\frac{\partial S}{\partial \theta_j}\right)^n \frac{\partial \theta_j}{\partial x} \cdots \tag{29}$$

Equation (29) is approximated by

$$S^{n+1} = S^n + \left(\frac{\partial S}{\partial \theta_j}\right)^n \Delta\theta_j^{n+1} \tag{30}$$

Substitution into equation (28) and rearrangement generates the following system of equations

$$\sum_j CCC_{kj}\, \Delta\theta_j^{n+1} = P_k \tag{31}$$

where

$$CCC_{kj} = CC_{kj} - \omega\, \Delta x \left\{ \left(\frac{u_{ex}}{u_e}\right)^{n+1} EF_{kj} - (u_e)^{n+1} AA_{kj} \tau_j^2 \right\}$$

and

$$P_k = \Delta x \left[\left\{ \omega \left(\frac{u_{ex}}{u_e}\right)^{n+1} + (1-\omega) \left(\frac{u_{ex}}{u_e}\right)^n \right\} \sum_j EF_{kj}\theta_j^n + \{\omega u_e^{n+1} + (1-\omega) u_e^n\} \sum_j AA_{kj}\tau_j^n \right]$$

Equations (31) are tridiagonal for linear elements and pentadiagonal for quadratic elements. Equations (31) are solved at each x^n step using a generalized Thomas algorithm. The generalized Thomas algorithm is able to take advantage of the profile of CCC when quadratic elements are used. That is, every other row of CCC is tridiagonal corresponding to a midside node at which the equation is generated. Consequently the execution time is not very much greater for quadratic than for linear elements (see Section 4).

It has been found to be more efficient to solve equations (31) *without iteration* and, if necessary, to restrict the step-size, Δx, than to iterate at each x^n location. A variable step-size, Δx, has been used. The criterion for changing the step-size is as follows. For the node at the wall, the change in the solution, $\Delta\theta_w^{n+1}/\theta_w^n$, is computed. If $\Delta\theta_w^{n+1}/\theta_w^n > \gamma$ the step-size is halved, if this is not less than the minimum step-size. If $\Delta\theta_w^{n+1}/\theta_w^n > 0{\cdot}1\gamma$ the step-size is increased by 50 per cent if this is not greater than the maximum step-size.

The original Dorodnitsyn formulation (Section 2.1) imposes the boundary condition $T = 0$ at $u = 1$ but imposes no boundary condition at $u = 0$. However a boundary condition for T can be obtained from equation (2). This is

$$T_u^2 = -2u_{ex}/u_e^2 \tag{32}$$

To impose this boundary condition it is convenient to make use of the *group finite element*

formulation[17] for T^2. Thus the following trial solution is introduced,

$$T^2 = \sum_j N_j T_j^2 \tag{33}$$

where $T_j = (1-u_j)\tau_j$. Using equations (32) and (33), $\Delta\theta_1^{n+1}$ can be eliminated from equation (31) and θ_1^{n+1}, τ_1^{n+1} obtained subsequently.

However, numerical experiments indicated that the accuracy of the solution (τ, C_f, δ etc.) was generally inferior to that when equation (32) was not imposed (Figure 3). A similar reduction in accuracy was experienced when equation (32) was used with the Dorodnitsyn spectral formulation. For the results presented in the rest of this paper equation (32) has *not* been used, unless otherwise stated.

3. CONVERGENCE PROPERTIES

In this section we examine the convergence properties of the Dorodnitsyn finite element formulation. Most of the results will be obtained for the error in T in the L_2 norm, i.e.

$$\|T-T_{ex}\|_2 = \left[\int_0^1 (T-T_{ex})^2\,du\right]^{1/2} \tag{34}$$

Additionally the convergence of the engineering parameters, skin friction, c_f, and displacement thickness, δ, is considered.

For the Falkner–Skan family of problems, the solution, T_{ex}, can be computed aribtrarily accurately following the procedure given by Cebeci and Bradshaw.[2] The Falkner–Skan family of problems is characterized by different values of β corresponding to different outer velocity distributions of the form

$$u_e = x^{\beta/(2-\beta)} \tag{35}$$

Three cases have been considered, with values $\beta = 0$, 0·5 and −0·15. these cases correspond to a flat plate (zero pressure gradient), favourable pressure gradient and an unfavourable pressure gradient, respectively. Because of the particular choice of u_e in equation (35), equations (3) and (4) can be reduced to an ordinary differential equation

$$F_{YYY} + FF_{YY} + \beta[1-(F_Y)^2] = 0 \tag{36}$$

where

$$Y = \eta((2-\beta)u_e x)^{1/2} \quad \text{and} \quad F_Y = u$$

Appropriate boundary conditions are F, $F_Y = 0$ at $y = 0$ and $F_Y = 1$ at $y = \infty$. Solutions to equation (36), using a fourth-order Runge–Kutta scheme with $\Delta Y = 0{\cdot}02$, have been obtained and used as the 'exact' solutions in the convergence results presented in Figures 2–9.

The variation of the L_2 error in T with the mesh size, Δu, have been computed for linear and quadratic elements by integrating from $1 \leqslant x/L \leqslant 9$ with the step-size, Δx, sufficiently small that all errors are due to the discretization in u. The convergence results shown in Figures 2 to 5 were obtained at $x/L = 6{\cdot}0$. However a qualitatively similar variation with Δu, and Δx, is obtained at all values of x/L.

For the zero pressure gradient case, $\beta = 0$, the velocity distribution at the outer edge of the boundary layer has no effect. The error in T in the L_2 norm, equation (34), with various Δu is shown in Figure 2. Also shown in Figure 2 are lines corresponding to convergence like $(\Delta u)^2$ and $(\Delta u)^3$.

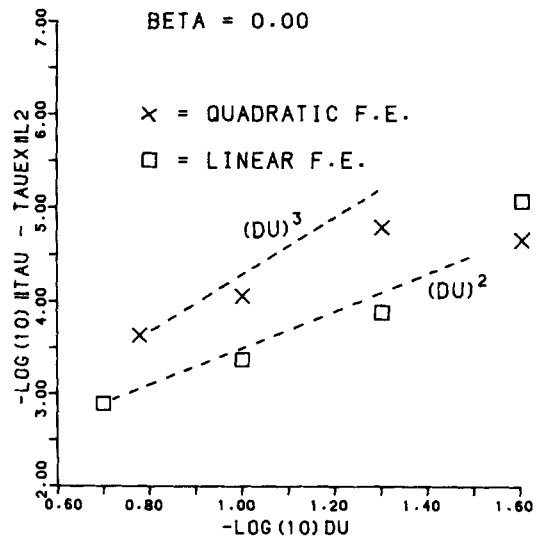

Figure 2. Variation of the L_2 error in T with Δu; $\beta = 0$

For linear elliptic problems, and linear parabolic problems with smooth initial conditions, theoretical estimates of the convergence rate for finite element formulations are available.[18] The theoretical results indicate that using linear elements produces second-order, $(\Delta u)^2$, convergence in the L_2 norm and using quadratic elements produces third-order convergence.

An examination of Figure 2 indicates that the use of linear elements achieves the theoretically expected second-order convergence. However the use of quadratic elements is only nominally second-order, if the result on the finest grid is ignored. However at levels of accuracy of practical interest, say $\Delta u = 0{\cdot}1$, the use of quadratic elements is *significantly more accurate* than the use of linear elements.

That the theoretically expected convergence rates are not achieved for quadratic elements is not completely unexpected. The present problem is highly non-linear and the simultaneous prescipition of Θ and T and the use of special trial functions is a significantly more complex situation than that for which the theoretical results were established.

Convergence properties for $\beta = 0{\cdot}5$ are shown in Figure 3. $\beta = 0{\cdot}5$ corresponds to a favourable pressure gradient. It is clear that the theoretical convergence rates are not achieved for either linear or quadratic elements. However this appears to be due, in part, to the relatively high accuracy that is achieved *on a coarse grid.*

Included in Figure 3 are convergence results with the wall boundary condition, equation (32), imposed. It is apparent that the convergence rate is lower than when the wall boundary condition is not enforced. Except for the coarsest grid the accuracy is *always lower* when the wall boundary condition is imposed.

An unfavourable pressure gradient, i.e. a flow condition that is retarding the flow, is provided by the case, $\beta = -0{\cdot}15$. Convergence results for this case are shown in Figure 4. Both linear and quadratic elements demonstrate second-order convergence except for quadratic elements on the finest grid.

For all three pressure gradient cases ($\beta = 0$, $0{\cdot}5$ and $-0{\cdot}15$) quadratic elements are more accurate than linear elements except for $\beta = 0$ and $-0{\cdot}15$ on the finest grid considered.

For linear problems the numerical integration scheme, equation (28), is second-order in Δx if $w = 0{\cdot}5$. However for the present non-linear problem the convergence is of lower order

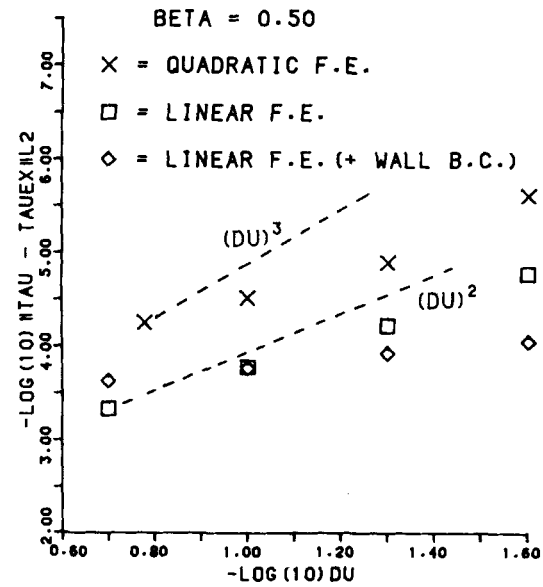

Figure 3. Variation of the L_2 error in T with Δu; $\beta = 0{\cdot}5$

(Figure 5). These results were obtained with linear finite elements and $\Delta u = 0{\cdot}025$. Consequently the errors in the solution are due to the x discretization when Δx is large and due to the u discretization when Δx is small. Thus for Δx small the error does not reduce with further reductions in Δx.

From a practical point of view the convergence of the skin friction, C_f, and the displacement thickness, δ/L, are of interest. The skin friction is a local property and related to the solution, T by

$$C_f = \frac{2}{Re^{1/2}} T_{u=0} \tag{37}$$

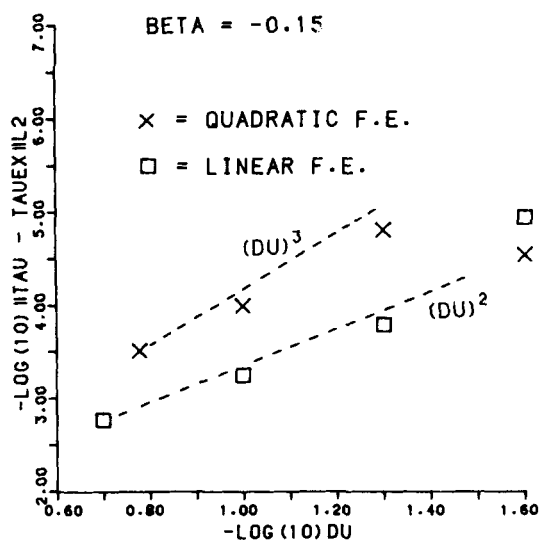

Figure 4. Variation of the L_2 error in T with Δu; $\beta = -0{\cdot}15$

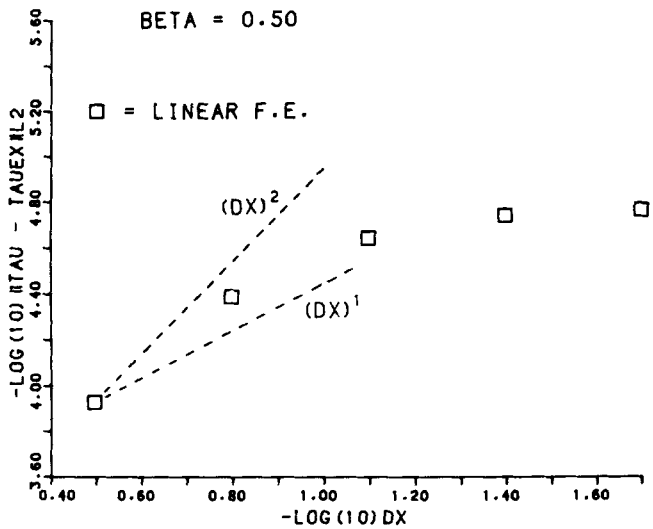

Figure 5. Variation of the L_2 error in T with Δx; $\beta = 0{\cdot}5$

The displacement thickness measures the reduction in mass flow, compared with the flow outside the boundary layer. It is defined by

$$\frac{\delta}{L} = \frac{1}{Re^{1/2} U_e} \int \frac{(1-u)}{\mathrm{T}} \, du \tag{38}$$

Like the L_2 error in T it is an integral property.

Figure 6 shows the variation of the rms error in $(C_f/C_{fex} - 1)$ and $(\delta/\delta_{ex} - 1)$ with Δx. The rms error has been computed over $16x/L$ values in the range $1 \leqslant x/L \leqslant 9$. This avoids the problem of picking a particular x/L at which, fortuitously, $C_f = C_{fex}$ or $\delta = \delta_{ex}$.

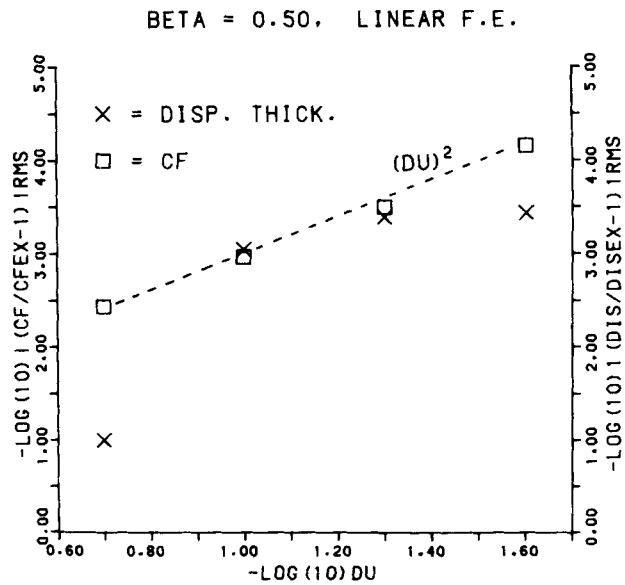

Figure 6. Variation of the error in skin friction, CF, and displacement thickness, DIS, with Δu; $\beta = 0{\cdot}5$

The results indicate a convergence for the skin friction that is *almost second-order*. The convergence for the displacement thickness is more uneven. However the results indicate that accuracies of the order of 0·1 per cent are obtained on a uniform grid of eleven points spanning the boundary layer.

The results for the convergence of skin friction and displacement thickness show the same trend that was apparent for T. That is, although high rates of convergence are not indicated, *the accuracy with a relatively coarse grid is very high.*

4. COMPUTATIONAL EFFICIENCY

The results shown in Figures 2–6 indicate that solutions of high accuracy can be obtained for all the pressure gradient cases on a relatively coarse grid of 11 points. Consequently the computational efficiency has been assessed by obtaining solutions with this distribution of grid points across the boundary layer but with a *coarser mesh* in the downstream, x, direction.

The results presented in this section have used a value of the step-size control parameter, $\gamma = 0{\cdot}10$. In practice the step-size, Δx, increases in the downstream direction *more rapidly* if γ is larger.

Typical solutions obtained with the Dorodnitsyn finite element formulation are compared with solutions obtained with the Dorodnitsyn spectral formulation and with a three-point finite difference scheme applied to equations (3) and (4).

The finite difference scheme is obtained in the following way. Equation (4) is written

$$u_j^n \, \Delta u_j^{n+1} = \Delta x(\omega S^{n+1} + (1-\omega)S^n) \tag{39}$$

i.e. in the same form as equation (28). In equation (39) S is given by

$$S = u_e u_{ex} + (u_{j-1} - 2u_j + u_{j+1})/Re \, \Delta^2 y - (u_{j+1} - u_{j-1})v_j/2 \, \Delta y \tag{40}$$

Linearizing S^{n+1} about the nth x level with v_j frozen produces an equation like (31), i.e.

$$\sum_{j=k-1}^{k+1} CCC_{kj} \, \Delta u_j^{n+1} = P_k \tag{41}$$

where

$$CCC_{kk-1} = -\omega(\psi + \lambda), \qquad CCC_{kk} = u_i^n + 2\psi\lambda$$
$$CCC_{kk+1} = \omega(\psi - \lambda), \qquad \psi = v_j^n \, \Delta x/2 \, \Delta y, \qquad \lambda = \Delta x/Re \, \Delta^2 y$$

and

$$P_k = \Delta x \, [\omega(u_e u_{ex})^{n+1} + (1-\omega)(u_e u_{ex})^n] + \lambda[u_{i-1}^n - 2u_i^n + u_{i+1}^n] - \psi[u_{i+1}^n - u_{i-1}^n]$$

The system of equations, (41), is solved in the same manner as equations (31). However at each x^n step it is necessary to obtain v_j^{n+1} from the discretized form of equation (3), i.e.

$$v_j^{n+1} = v_{j-1}^n - \frac{\Delta y}{2 \, \Delta x}[u_j^{n+1} - u_j^n + u_{j-1}^{n+1} - u_{j-1}^n] \tag{42}$$

We expect solutions of equations (41) and (42) to be of order $(\Delta^2 y, \Delta x)$ i.e. comparable to the use of linear elements in equation (31).

A summary of the results obtained with a quadratic finite element formulation and the implicit finite difference formulation are shown in Table I. The algorithms used to integrate

Table I. Execution time comparison of the finite element and finite difference methods

	Zero pressure gradient, $\beta = 0$		Favourable pressure gradients $\beta = 0{\cdot}5$		Unfavourable pressure gradient $\beta = -0{\cdot}15$	
	Finite element	Finite difference	Finite element	Finite difference	Finite element	Finite difference
Gridpoints across boundary layer	11	41	11	41	11	41
Number of steps, $\Delta x/L$	95	94	123	109	88	125
$\Delta x/L$	0·01 to 0·256	0·01 to 0·256	0·01 to 0·171	0·01 to 0·076	0·01 to 0·256	0·01 to 0·171
Relative execution time	1·00	5·00	1·32	3·89	1·00	5·26

the equations downstream are similar and require approximately the same number of steps and cover the same range of step-sizes. In fact both methods use the same algorithm for changing the step-size. However the finite element formulation is typically 3 to 5 times *more economical.* This economy follows from the fewer grid points across the boundary layer required by the Dorodnitsyn finite element formulation.

However to compare the computational efficiency of the finite element and finite difference methods it is also necessary to compare the accuracy of the two methods. This has been done for $\beta = 0$, 0·5 and −0·15 in Figures 7–9, respectively. The basis of the comparision to consider the skin friction and displacement thickness variation over the range $1{\cdot}0 \leqslant x/L \leqslant 9{\cdot}0$. The exact variation of the skin friction and displacement thickness for the zero pressure gradient case is shown in Figure 7(a); only sufficient points have been shown to indicate the variation with x.

The percentage errors in the skin friction and displacement thickness are shown in Figures 7(b) and 7(c), respectively. Also shown in Figures 7(b) and 7(c) are solutions obtained with the Dorodnitsyn spectral method (Section 2.2) with four unknown coefficients in equation (17). It is clear that all three methods are producing solutions of *comparable accuracy.* For this case u_{ex}, in equation (4), is zero.

The exact solutions for the favourable pressure gradient case is shown in Figure (8a). The corresponding errors shown in Figures (8b) and (8c) indicate that all three methods are achieving a high accuracy. However the spectral method demonstrates a large initial perturbation away from the exact solution. This effect is apparent in other spectral results[15] and appears to be related to an incompatibility of the spectral method with the form of the initial data.

For an unfavourable pressure gradient, $\beta = -0{\cdot}15$, the skin friction is small for all values of x/L and the displacement thickness grows rapidly with x/L (Figure 9(a)). The errors in skin friction for the various methods are shown in Figure 9(b). It is clear that all methods are of comparable accuracy. Although the percentage errors are considerably larger than for $\beta = 0{\cdot}5$ (Figure 8(b)) the absolute errors are of comparable magnitude. The percentage errors in the displacement thickness (Figure 9(c)) are also of a comparable magnitude to those for $\beta = 0{\cdot}5$.

If the accuracies shown in Figures 7 to 9 are considered along with the relative execution times shown in Table I then it is clear that the Dorodnitsyn finite element formulation is

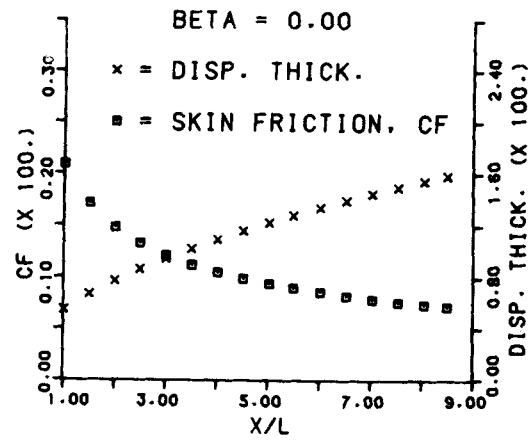

(a)

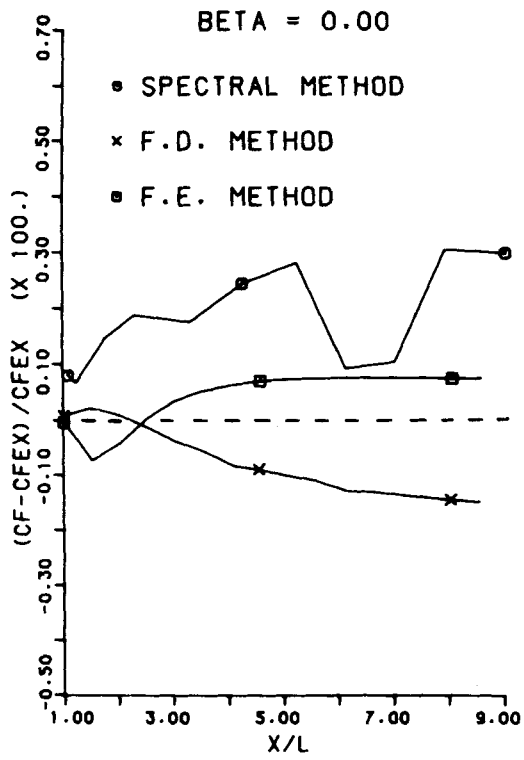

(b)

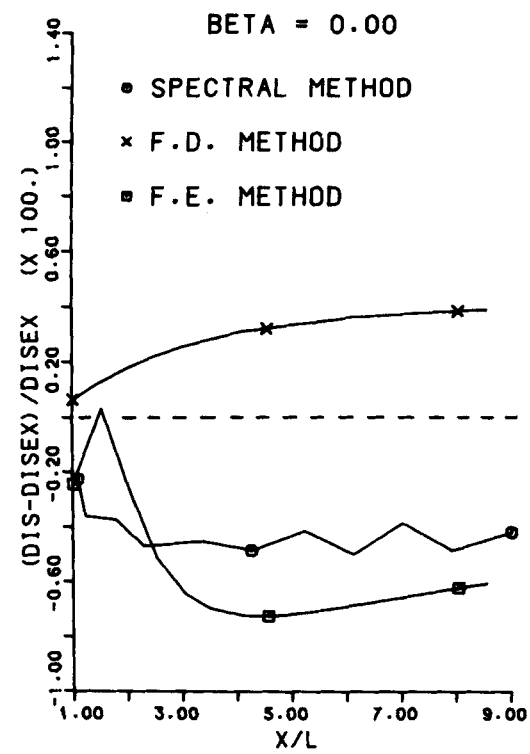

(c)

Figure 7. Comparison of the Dorodnitsyn finite element, Dorodnitsyn spectral and a finite difference method for zero pressure gradient, $\beta = 0$: (a) exact solution; (b) percentage error in skin friction; (c) percentage error in displacement thickness

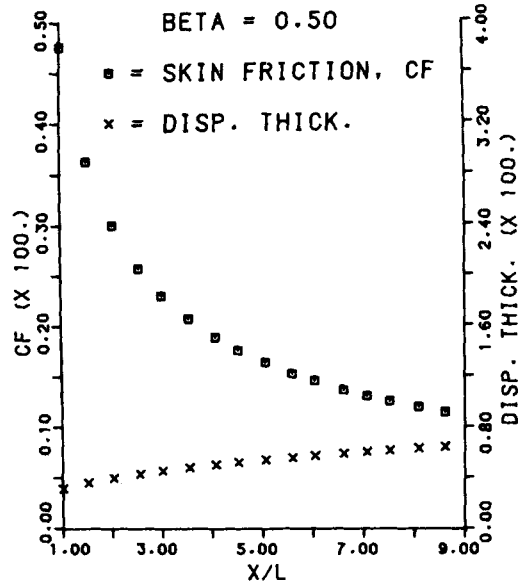

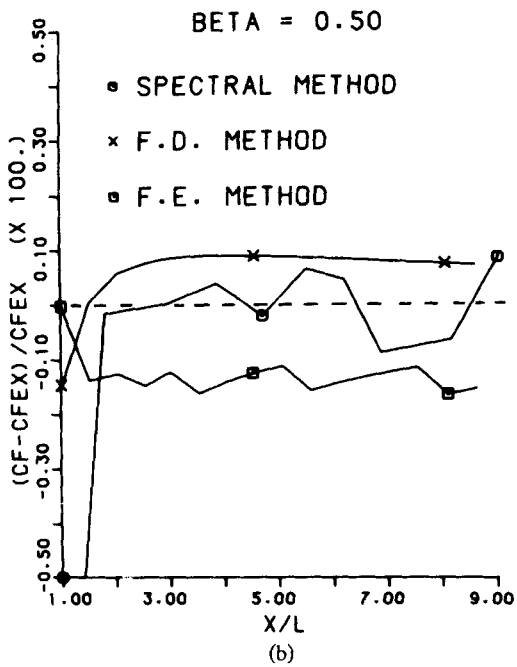

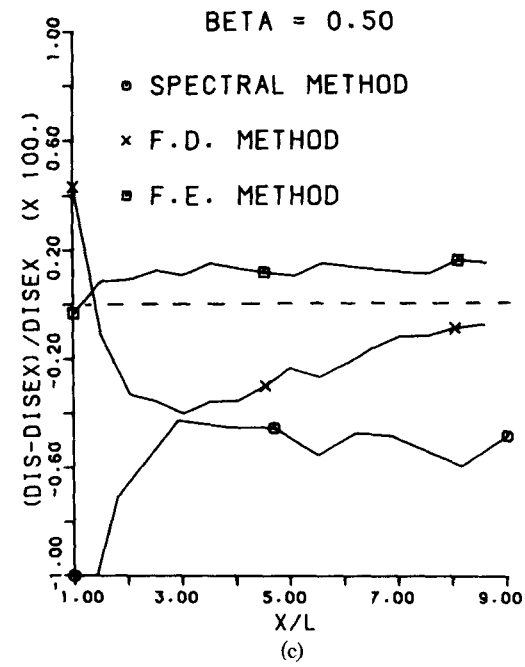

Figure 8. Comparison of the Dorodnitsyn finite element., Dorodnitsyn spectral and a finite difference method for a favourable pressure gradient, $\beta = 0{\cdot}50$: (a) exact solution; (b) percentage error in skin friction; (c) percentage error in displacement thickness

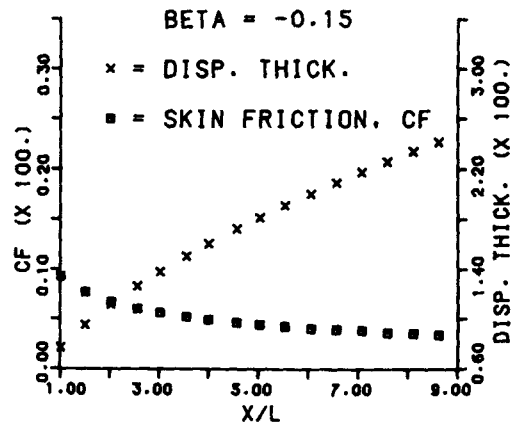

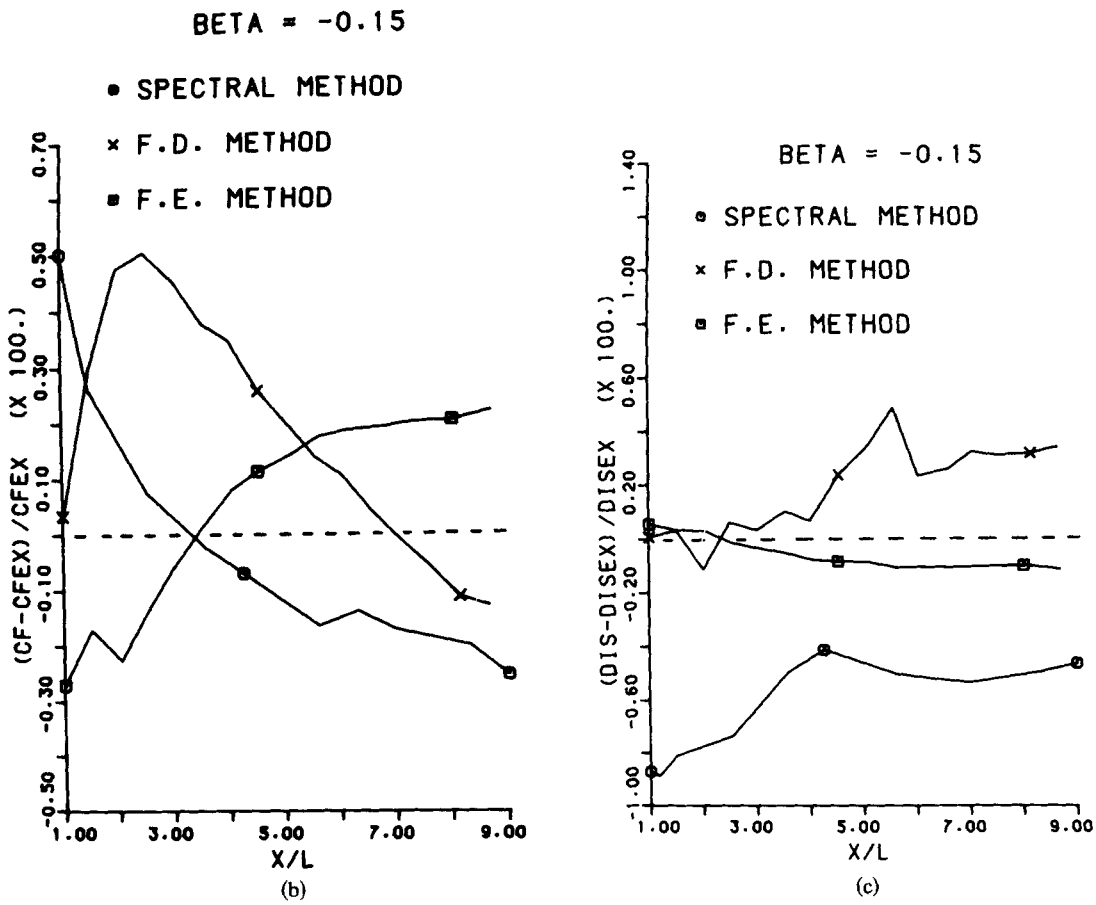

Figure 9. Comparison of the Dorodnitsyn finite element, Dorodnitsyn spectral and a finite difference method for an adverse pressure gradient, $\beta = -0{\cdot}15$: (a) exact solution; (b) percentage error in skin friction; (c) percentage error in displacement thickness

computationally more efficient than the implicit finite difference formulation for the boundary layer equations. *Even more substantial increases* in computational efficiency have been found when the Dorodnitsyn finite element formulation is applied to turbulent boundary layers.[11]

5. FLOW OVER A CIRCULAR CYLINDER

This application is included because it features an initially favourable pressure gradient (up to $\phi = 90°$) and an unfavourable pressure gradient beyond $\phi = 90°$. Eventually separation occurs. The ability of a boundary layer method to predict separation is an important property.

At separation the shear stress at the surface becomes zero. In the present formulation this corresponds to $\tau_w = 0$. However this also corresponds to $\theta_w = \infty$. The form of equation (31) is not suitable close to separation since it generates large values for $\Delta\theta_w$ etc.

However, it is straightforward to formulate the equivalent equation that gives $\Delta\tau$, the correction to τ, in place of equation (31). That is, equation (27) can be written

$$-\sum_j \frac{CC_{kj}}{\tau_j^2}\frac{d\tau_j}{dx} = \frac{u_{ex}}{u_e}\sum_j EF_{kj}/\tau_j + u_e \sum_j AA_{kj}\tau_j \tag{39}$$

Since τ_w will reach zero before any other value of τ, it is convenient to multiply by τ_{k-1}^2 (for linear elements). Then equation (39) becomes

$$-\sum_j CC_{kj}\frac{\tau_{k-1}^2}{\tau_j^2}\frac{d\tau_j}{dx} = \frac{u_{ex}}{u_e}\sum_j EF_{kj}\tau_{k-1}^2/\tau_j + u_e \sum_j AA_{kj}\tau_{k-1}^2\tau_j \tag{40}$$

Equation (40) is valid, and works effectively, *right up to separation.* Beyond separation the

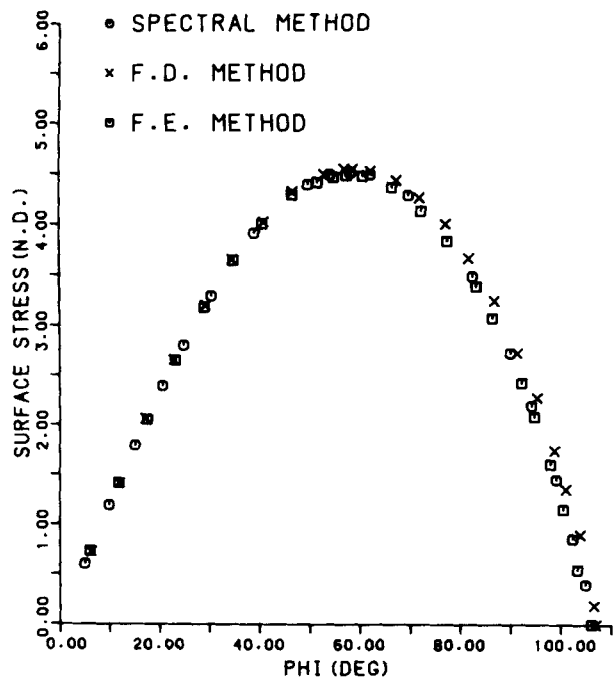

Figure 10. Shear stress variation at the surface of a circular cylinder

boundary layer equation as given above, equation (11), is not valid. However if the interval $0<u<1$ is replaced by two intervals, $u_{min}<u<0$ and $u_{min}<u<1$, a unique relationship between u and y can still be obtained. This approach has been developed for the traditional method of integral relations,[7] but is not pursued here.

A typical surface shear stress distribution with ϕ is shown in Figure 10. The finite element results were obtained with quadratic elements, $\Delta u = 0{\cdot}10$ and $0{\cdot}001 \leqslant \Delta\phi \leqslant 0{\cdot}064$. These results are compared with those obtained with a four-term spectral method and the finite difference method described previously. The finite difference scheme used 41 points across the boundary layer. A similarity stagnation point solution, $\beta = 1{\cdot}0$ in equation (35), is used as starting data for all the methods. It can be seen that all methods are in close agreement except near to separation.

The corresponding variation of displacement thickness is shown in Figure 11. As with the surface shear stress results, agreement is better in the favourable pressure gradient region than in the region close to separation. Velocity distributions for angles $\phi = 40°$ and $80°$ are shown in Figure 12. Agreement between the methods is better at 40° than at 80°.

For this problem the Dorodnitsyn finite element formulation predicts a separation point of $\phi = 106{\cdot}1°$. This compares with a value of 105° due to Cebeci and Bradshaw.[2] The Dorodnitsyn spectral method used the equivalent of equation (27). Close to separation the variable-step algorithm generated smaller and smaller steps, $\Delta\phi$, presumably due to the growth in θ_w. Consequently it was necessary to curtail this integration prior to separation. The finite difference scheme predicted separation at $\phi = 106{\cdot}9°$.

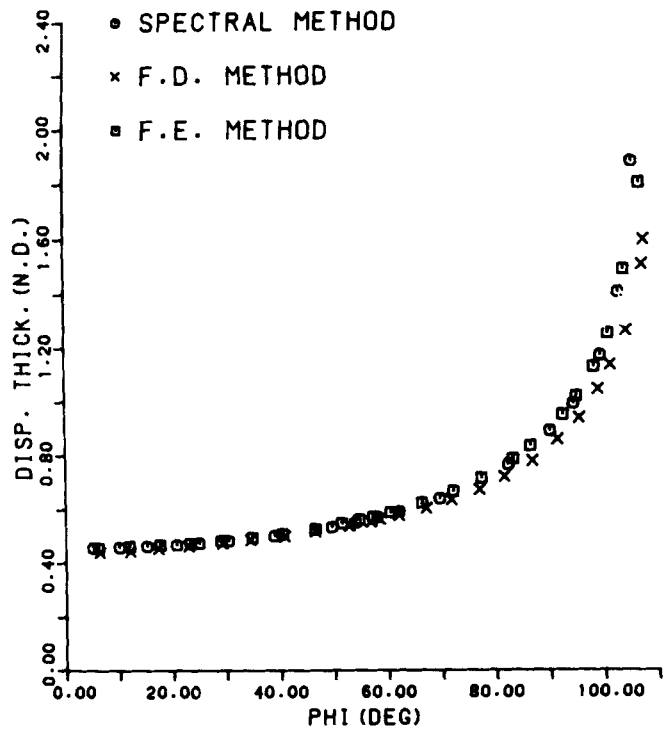

Figure 11. Variation in displacement thickness for flow over a circular cylinder

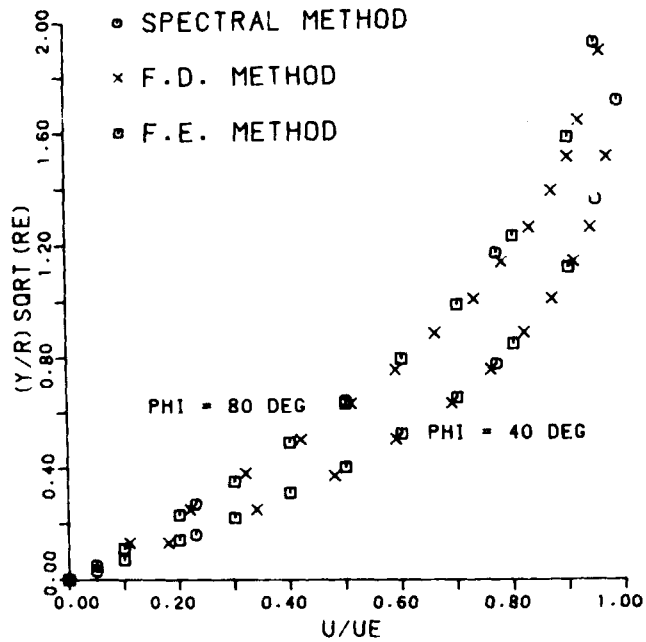

Figure 12. Typical boundary layer velocity profiles for flow over a circular cylinder

6. CONCLUSIONS

The Dorodnitsyn boundary layer formulation provides a *high resolution* across the boundary layer, avoids the explicit appearance of the normal velocity, v, and obtains solutions for the skin friction directly.

We have shown that the Dorodnitsyn formulation can be given a finite element interpretation by an *appropriate* choice of test and trial functions. When combined with an implicit, non-iterative marching scheme in the downstream direction an algorithm is obtained that is both highly accurate and economical.

The algorithm has been tested on the Falkner–Skan family of laminar boundary layer problems. The algorithm is of order $(\Delta^2 u, \Delta x)$ whether linear or quadratic elements are used, but produces solutions of *high accuracy on coarse grids.*

The use of quadratic elements (in u) produces solutions of comparable accuracy to a three-point finite difference scheme but with only *one fifth of the execution time.*

With a small modification the Dorodnitsyn finite element formulation is able to give accurate solutions right up to separation.

REFERENCES

1. F. G. Blottner, 'Computational techniques for boundary layers', *AGARD Lecture Notes No. 73* (1975).
2. T. Cebeci and P. Bradshaw, *Momentum Transfer in Boundary Layers*, Hemisphere, 1977.
3. Z. Popinski and A. J. Baker, 'An implicit finite element algorithm for the boundary layer equations', *J. Comp. Phys.*, **21**(1) 55–84 (1976).
4. M. O. Soliman and A. J. Baker, 'Accuracy and convergence of a finite element algorithm for laminar boundary layer flow', *Comp. and Fluids*, **9**, 43–62 (1981).
5. M. O. Soliman and A. J. Baker, 'Accuracy and convergence of a finite element algorithm for turbulent boundary layer flow', *Comp. Math. Appl. Mech. Eng.*, **28**, 81–102 (1981).

6. A. A. Dorodnitsyn, 'General method of integral relations and its application to boundary layer theory', *Adv. Aero. Sci.*, **3,** 207–219 (1962).
7. M. Holt, *Numerical Methods in Fluid Dynamics*, Springer-Verlag, 1977.
8. C. A. J. Fletcher, *Computational Galerkin Methods*, Springer-Verlag, 1983.
9. C. A. J. Fletcher and M. Holt, 'An Improvement to the Method of Integral Relations', *J. Comp. Phys*, **18,** 154–164 (1975).
10. C. A. J. Fletcher, 'Application of an improved method of integral relations to the supersonic boundary layer flow about cones at large angles of attack' in J. Noye (ed.) *Numerical Simulation of Fluid Motion*, North-Holland, 537–550 (1978).
11. C. A. J. Fletcher and R. W. Fleet, 'The Dornodnitsyn finite element formulation for turbulent boundary layers', *Computers and Fluids* (to appear, 1983).
12. E. Isaacson and H. B. Keller, *Analysis of Numerical Methods*, Wiley, 1966.
13. C. W. Gear, *Comm. A.C.M.*, **14,** 176–179 (1971).
14. C. A. J. Fletcher and M. Holt, 'Supersonic flow about inclined cones', *J. Fluid Mech.*, **74,** 561–591 (1976).
15. W-S. Yeung and R-J. Yang, 'Application of the method of integral relations to the calculation of two-dimensional incompressible turbulent boundary layers', *J. Appl. Mech.*, **48,** 701–706 (1981).
16. W. R. Briley and H. McDonald, 'Solution of the multi-dimensional compressible Navier–Stokes equations by a generated implicit method', *J. Comp. Phys.*, **24,** 372–397 (1977).
17. C. A. J. Fletcher, 'The group finite element formulation', *Comp. Meth. Appl. Mech. Eng.* **37,** 225–243 (1983).
18. J. T. Oden and J. N. Reddy, *An Introduction to the Mathematical Theory of Finite Elements*, Wiley, 1976.